Constraining the non-thermal emission site and geometry of AR Sco via optical polarimetry.

Louis Du Plessis

Supervisors: C. Venter
Z. Wadiasingh
A.K. Harding

Centre for Space Research North-West University

September 10, 2021

AR Sco Observations

- Marsh et al. (2016) detected optical and radio pulsations from the binary white dwarf (WD) system AR Scorpii
- Orbital period of 3.55 hours and a "pulsar" spin period of 1.95 min
- Constrained the mass of the WD to $\sim 0.8 M_{\odot}$ and the M-dwarf companion to $\sim 0.3 M_{\odot}$
- Stiller et al. (2018) obtained a $\dot{P} = 7.18 \times 10^{-13}\ ss^{-1}$

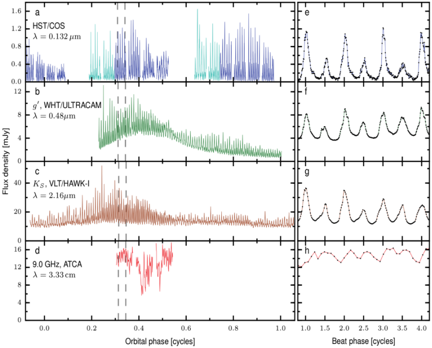

Figure: Light Curve of AR Sco from Marsh et al. (2016) showing ultraviolet to radio bands

AR Sco Observations

- Optical and UV emission lines show no indication of an accretion disc
- The optical and UV are non-thermal emission and pulsed at the WD spin period
- This gives a light cylinder radius of $R_{\mathrm{LC}} = 5.6 \times 10^{11}$ *cm* and an orbital semi-major axis of $a = 8.5 \times 10^{10}$ *cm*
- Buckley et al. (2017) found that the system exhibits strong linear optical polarisation (up to $\sim 40\%$) and the WD having a magnetic field estimated to be $\sim 500\mathrm{MG}$

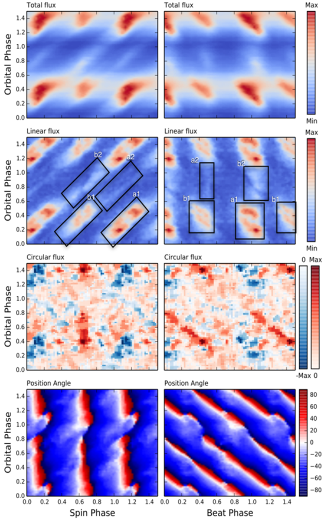

Figure: Extensive observational data from Potter and Buckley (2018)

AR Sco Observations

- Garnavich et al. (2020) detected two hotspots located at the poles of the WD.
- Garnavich et al. (2020) inferred an upper limit of $100\mathrm{MG}$ for the WD surface field using Zeeman splitting.
- Takata et al. (2020) found a double-peaked structure in the X-rays vs. the single-peaked structure observed in the 2016 and 2018 observations.

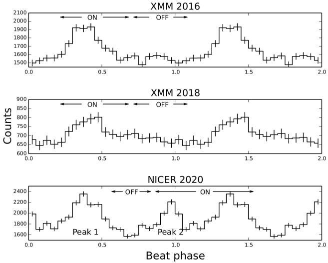

Figure: Takata et al. (2020)

AR Sco Observations

- Takata et al. (2020) created phase maps of the X-ray pulse profiles, folded at with the beat and spin period, respectively.
- Some components of the emission were found to be coupled to the beat period and others to the spin period.
- *Fermi LAT* analysis done by Kaplan et al. (2019) and Singh et al. (2020) showed a 2σ detection for γ-rays from the source.

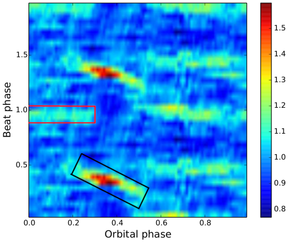

Figure: Takata et al. (2020)

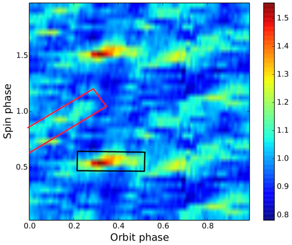

Figure: Takata et al. (2020)

AR Sco Observations

System Illustration

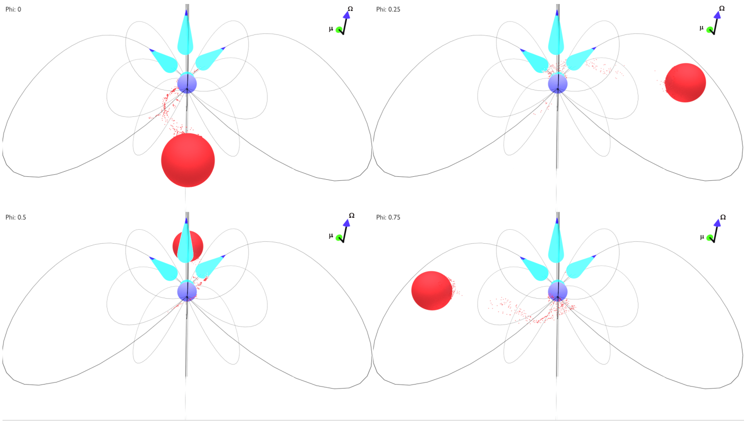

Model Descriptions

- **Shock front emission models**
  - Geng et al. (2016) shock accelerated-particles model.
  - Katz et al. (2017) precession model.
  - Garnavich et al. (2018) magnetic reconnection model.
  - Bednarek (2018) hadronic model.
- **WD magnetospheric emission models**
  - Buckley et al. (2017) spin-down pulsar model.
  - Takata et al. (2017) magnetic mirror model.
  - Potter & Buckley (2018) particle injection model (Geometric).
  - Du Plessis et al. (2019) RVM (Geometric).
  - Lyutikov et al. (2020) ionised plasma model.
- **WD current-sheet model**

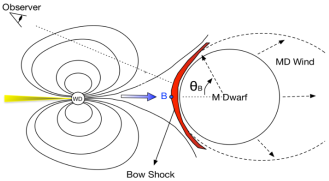

Figure: Geng et al.(2016)

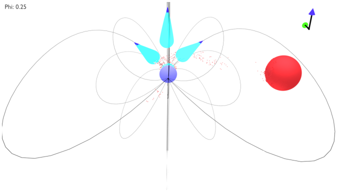

Shock Front Emission Models

- Geng et al. (2016)
  - Emission originating from interacting magnetic fields (hypothetical high-density bow-shock region).
  - No explanation for highly periodic emission or high degree of polarisation.
- Katz (2017)
  - Precession of the WD.
  - Enhanced heating on the leading face of the companion leading to asymmetric/precessing optical LC.
- Garnavich et al. (2018)
  - Magnetic reconnection model.
  - Expand on the Lyutikov et al. (2020) model.
- Bednarek (2018)
  - Hadronic and mixture of leptonic and hadronic model.
  - Only two ideal scenarios barely below *Fermi LAT* upper limits.

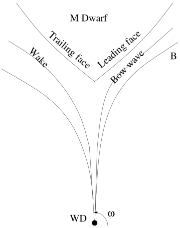

Figure: Katz (2017)

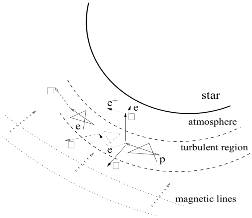

Figure: Bednarek (2018)

WD Magnetosphere Emission Models

- Buckley et al. (2017)
  - Spin-down powered WD pulsar model.
  - Can WD supply needed particles?
- Takata et al. (2017)
  - Magnetic mirror model with time-of-flight effects.
  - Use particle transport equations from Harding et al. (2005) which are derived under assumption of large Lorentz factor and small pitch angles.
  - Magnetic mirror scenario violates these conditions.
  - Different particle pitch angle populations.

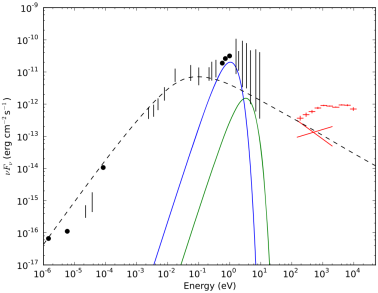

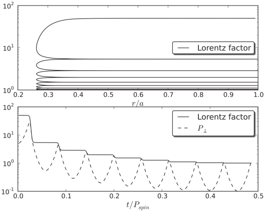

Figure: Takata et al. (2017)

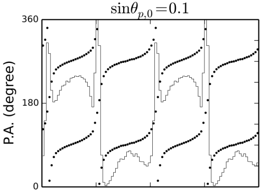

Figure: Takata et al. (2019)

WD Magnetosphere Emission Models

- Potter and Buckley (2018)
  - Geometric model that uses magnetic mirror idea to reproduce their observed phase plots.
  - Particles injected at specific part of orbital phase at cool via SR.
- Du Plessis et al. (2019)
  - Applied rotating vector model.
- Singh et al. (2020)
  - Two particle population Synchrotron model, only modelling the SED.
- Lyutikov et al. (2020)
  - Intermediate Polar model.
  - No indication of accretion column.

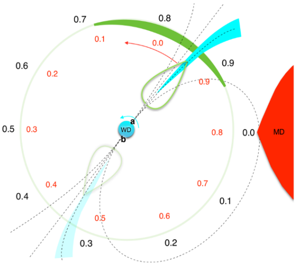

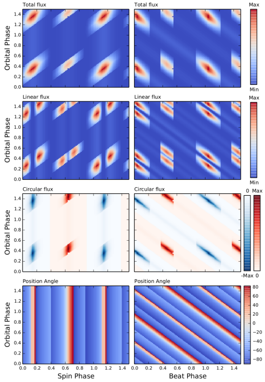

Figure: Potter and Buckley (2018)

Du Plessis et al. in prep (2021)

- We fit our standard RVM to the orbitally-binned PPA data from Potter and Buckley (2018).
- Blue is the beat-folded linear flux
- Red is the spin-folded linear flux
- Linear flux maximum between orbital phase 0.2 – 0.45
- Mixture of spin- and beat-coupled emission

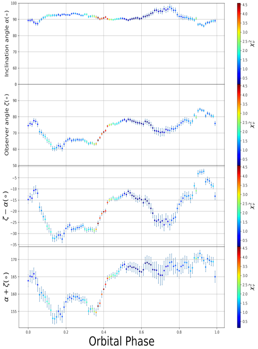

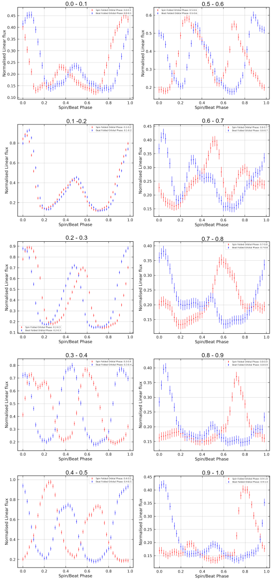

Variation in α and ζ Speculations

- Precession of the WD.
- Biased orbital sampling.
- Asymmetric or wobbling emissions region.
- Different particle pitch angles.
- Different injection regions and rates.
- A mix of WD and companion emission might have an effect on orbitally-dependent depolarization.

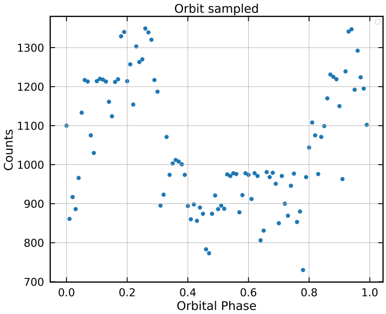

Future Applications

- Develop a more sophisticated emission model.
- Start with static dipole field, no mirror, and no $\mathbf{E} \times \mathbf{B}$ drift.
- Solve the coupled transport equations from Harding et al. (2005) more generally without assuming $\gamma \gg 1$ and small pitch angles.
- Produce orbital phase-resolved light curves, spectra, polarisation position angle, and polarisation degree vs WD spin.

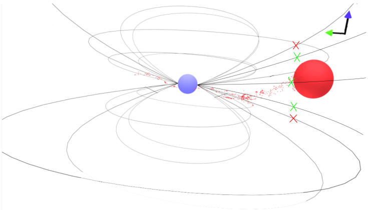

- Introduce $\mathbf{E} \times \mathbf{B}$ drift and particle turnaround.
- Introduce time dependant particle injection.
- Investigate particle turnaround point, injection scenarios, and magnetic field structure.

Bibliography

Buckley, D. A. H., Meintjes, P. J., Potter, S. B., Marsh, T. R., and Gänsicke, B. T. (2017). Polarimetric evidence of a white dwarf pulsar in the binary system AR Scorpii. *Nature Astronomy*, 1:0029.

Harding, A. K., Usov, V. V., and Muslimov, A. G. (2005). High-energy emission from millisecond pulsars. *The Astrophysical Journal*, 622(1):531.

Marsh, T. R., Gänsicke, B. T., Hümmerich, S., Hambsch, F.-J., Bernhard, K., Lloyd, C., Breedt, E., Stanway, E. R., Steeghs, D. T., Parsons, S. G., Toloza, O., Schreiber, M. R., Jonker, P. G., van Roestel, J., Kupfer, T., Pala, A. F., Dhillon, V. S., Hardy, L. K., Littlefair, S. P., Aungwerojwit, A., Arjyotha, S., Koester, D., Bochinski, J. J., Haswell, C. A., Frank, P., and Wheatley, P. J. (2016). A radio-pulsing white dwarf binary star. *Nature Astronomy*, 537:374–377.

Potter, S. B. and Buckley, D. A. H. (2018). Time series photopolarimetry and modeling of the white dwarf pulsar in AR Scorpii. *Mon. Not. Roy. Astron. Soc.*

Stiller, R. A., Littlefield, C., Garnavich, P., Wood, C., Hambsch, F.-J., and Myers, G. (2018). High-Time-Resolution Photometry of AR Scorpii: Confirmation of the White Dwarf's Spin-Down. *ArXiv e-prints*.